Does Histidine 332 of the D1 Polypeptide Ligate the Manganese Cluster in Photosystem II? An Electron Spin Echo Envelope Modulation Study†

Richard J. Debus,*,‡ Kristy A. Campbell,§,|| Wolfgang Gregor,§ Zhao-Liang Li,⊥ Robert L. Burnap,⊥ and R. David Britt*,§

Department of Biochemistry, University of California, Riverside, California 92521-0129, Department of Chemistry, University of California, Davis, California 95616, and Department of Microbiology and Molecular Genetics, Oklahoma State University, Stillwater, Oklahoma 74078

Received October 16, 2000; Revised Manuscript Received January 30, 2001

ABSTRACT: The tetranuclear manganese cluster in photosystem II is ligated by one or more histidine residues, as shown by an electron spin echo envelope modulation (ESEEM) study conducted with [^{15}N]histidine-labeled photosystem II particles isolated from the cyanobacterium *Synechocystis* sp. strain PCC 6803 [Tang, X.-S., Diner, B. A., Larsen, B. S., Gilchrist, M. L., Jr., Lorigan, G. A., and Britt, R. D. (1994) *Proc. Natl. Acad. Sci. U.S.A. 91*, 704−708]. One of these residues may be His332 of the D1 polypeptide. Photosystem II particles isolated from the *Synechocystis* mutant D1-H332E exhibit an altered S_2 state multiline EPR signal that has more hyperfine lines and narrower splittings than the corresponding signal in wild-type PSII particles [Debus, R. J., Campbell, K. A., Peloquin, J. M., Pham, D. P., and Britt, R. D. (2000) *Biochemistry 39*, 470−478]. These D1-H332E PSII particles are also unable to advance beyond an altered $S_2Y_Z^\bullet$ state, and the quantum yield for forming the S_2 state is very low, corresponding to an 8000-fold slowing of the rate of Mn oxidation by $Y_Z^\bullet$. These observations are consistent with His332 being close to the Mn cluster and modulating the redox properties of both the Mn cluster and tyrosine Y_Z. To determine if D1-His332 ligates the Mn cluster, we have conducted an ESEEM study of D1-H332E PSII particles. The histidyl nitrogen modulation observed near 5 MHz in ESEEM spectra of the S_2 state multiline EPR signal of wild-type PSII particles is substantially diminished in D1-H332E PSII particles. This result is consistent with ligation of the Mn cluster by D1-His332. However, alternate explanations are possible. These are presented and discussed.

The catalytic site for water oxidation in photosystem II (PSII)[1] contains four Mn ions plus the redox active tyrosine, Y_Z [for review, see (*1*−*9*)]. One Ca^{2+} ion and one Cl^- ion are required for catalytic activity and appear to be located in the vicinity of the Mn cluster. Recent simulations of EPR and ENDOR data show that the four Mn ions are arranged as a magnetically coupled tetramer probably consisting of a strongly exchange-coupled trinuclear core that is weakly exchange-coupled with a fourth Mn ion (*10*, *11*) [reviewed in (*12*, *13*)]. The exact arrangement of the Mn ions is unknown, even with the recent 3.8 Å structure of PSII (*14*). However, EXAFS studies detect the presence of two to three Mn−Mn distances of ∼2.7 Å and one Mn−Mn or Mn−Ca distance of ∼3.3 Å (*3*, *4*, *15*, *16*). These distances are consistent with the Mn ions being connected by μ_2-oxo, di-μ_2-oxo, or μ_3-oxo bridges (*3*, *4*, *15*, *16*).

The Mn cluster accumulates oxidizing equivalents in response to photoinduced electron-transfer reactions within PSII, and then catalyzes the oxidation of two molecules of water, releasing one molecule of O_2 as a byproduct. During each catalytic cycle, the Mn cluster cycles through five oxidation states termed S_n, where n denotes the number of oxidizing equivalents stored. The S_1 state predominates in dark-adapted samples. On the basis of XANES data, the S_1 state is believed to consist of two Mn(III) and two Mn(IV) ions, and the S_2 state is believed to consist of one Mn(III) and three Mn(IV) ions (*3*, *4*, *15*, *16*). The S_4 state is a transient intermediate that reverts to the S_0 state with the concomitant release of O_2. The photoinduced electron-transfer reactions that precede water oxidation take place in a heterodimer of two homologous polypeptides known as D1 and D2.

† This work was supported by the National Institutes of Health (GM43496 to R.J.D. and GM48242 to R.D.B.) and by the National Science Foundation (MCB 9728754 to R.L.B.).

* To whom correspondence should be addressed. R.J.D.: Phone (909) 787-3483, Fax (909) 787-4434, E-mail debusrj@citrus.ucr.edu. R.D.B.: Phone (530) 752-6377; Fax (530) 752-8995; Email rdbritt@ucdavis.edu.

‡ University of California, Riverside.

§ University of California, Davis.

|| Present address: Micron Technology, Inc., 8000 S. Federal Way, Boise, ID 83707-0006.

⊥ Oklahoma State University.

[1] Abbreviations: Chl, chlorophyll; DCMU, 3-(3,4-dichlorophenyl)-1,1-dimethylurea; DMSO, dimethyl sulfoxide; EPR, electron paramagnetic resonance; ESE, electron spin echo; ESEEM, electron spin echo envelope modulation; EXAFS, extended X-ray absorption fine structure; MES, 2-(*N*-morpholino)ethanesulfonic acid; NTA, nitrilotriacetic acid; P_{680}, chlorophyll species that serves as the light-induced electron donor in PSII; Pheo, pheophytin; PSII, photosystem II; Q_A, primary plastoquinone electron acceptor; wild-type*, control strain of *Synechocystis* sp. strain PCC 6803 constructed in identical fashion as the D1-H332E mutant, but containing the wild-type *psb*A-2 gene; Y_Z, tyrosine residue that mediates electron transfer between the Mn cluster and $P_{680}^{+\bullet}$; XANES, X-ray absorption near-edge structure.

10.1021/bi002394c CCC: $20.00
Published on Web 02/27/2001

The immediate oxidant of the Mn cluster is Y_Z, Tyr-161 of the D1 polypeptide. Simulations of EPR and ENDOR data obtained with samples trapped in the $S_2Y_Z^\bullet$ state show that the point−dipole distance between $Y_Z^\bullet$ and the Mn cluster is 7−9 Å (*17*−*23*), in agreement with the electron densities assigned to Y_Z and the Mn cluster in the recent 3.8 Å structure (*14*). This distance is compatible with structural models showing either direct hydrogen bonding between Y_Z and a water-derived Mn ligand (*5*, *8*, *24*−*27*) or indirect hydrogen bonding, such as via an intervening water molecule (*9*, *11*−*13*). Hydrogen bonding between Y_Z and the Mn cluster, whether direct or indirect, would be consistent with recent proposals for the mechanism of water oxidation that invoke proton-coupled electron transfer from Mn-bound water molecules or water-derived Mn ligands to $Y_Z^\bullet$ [reviewed in (*2*, *8*, *9*, *24*−*27*)].

Several lines of evidence suggest that the D1 polypeptide contributes most or all of the amino acid residues that coordinate the Mn and Ca ions in PSII [for review, see (*6*, *28*, *29*)]. The Mn ions are coordinated primarily by oxygen atoms (*30*−*33*), such as provided by μ-oxo bridges, carboxylate residues, peptide carbonyl groups, and water-derived ligands. Coordination by both carboxylate and histidine residues has been proposed on the basis of chemical modification studies (*34*−*42*). Coordination by at least one histidine residue has been demonstrated by an ESEEM study conducted with PSII preparations labeled with [^{15}N]histidine (*33*). This work extended earlier ESEEM (*30*, *32*) and ENDOR (*31*) studies that provided evidence of Mn ligation by at least one nitrogen atom. Subsequent ESEEM studies suggest that the ligating histidine residue(s) coordinate(s) Mn with their $\epsilon 2$ (τ) nitrogen(s) (*43*). Additional evidence for coordination by histidine was provided by a recent FTIR study conducted with [^{15}N]histidine (*44*). Coordination by a carboxylate residue that forms a bridge to a Ca ion has been proposed on the basis of an FTIR study of intact and Ca-depleted samples (*45*), although the bridging aspect of this assignment has been questioned (*46*, *47*). Site-directed mutagenesis studies have identified D1-Asp170 (*48*−*52*), D1-His190 (*52*−*55*), D1-His332 (*53*, *55*, *56*), D1-Glu333 (*53*, *55*, *56*), D1-His337 (*53*, *55*, *56*), D1-Asp342 (*53*, *55*, *56*), and the *C*-terminus of Ala344 (*57*) as potential ligands of the Mn cluster [for review, see (*6*, *28*, *29*)]. The residue D1-His337 has also been proposed to ligate the Mn cluster on the basis of chemical modification and protease digestion studies (*37*, *42*).

The ESEEM (*33*, *43*) and FTIR (*44*) studies showing that at least one histidine residue coordinates the Mn cluster in PSII have focused attention on D1-His190, D1-His332, and D1-His337. We previously presented a characterization of PSII particles isolated from the *Synechocystis* mutant D1-H332E (*58*). This mutant is of particular interest because it appears to assemble Mn clusters in nearly all reaction centers in vivo, but evolves no O_2 (*56*). In the previous study, we showed that D1-H332E PSII particles exhibit an altered S_2 state multiline EPR signal that has more hyperfine lines and narrower splittings than the corresponding signal in wild-type PSII particles. We also showed that D1-H332E PSII particles are unable to advance beyond an altered $S_2Y_Z^\bullet$ state, that the quantum yield for forming the S_2 state is very low, corresponding to an 8000-fold slowing of the rate of Mn oxidation by $Y_Z^\bullet$, and that the temperature threshold for forming the S_2 state is approximately 100 K higher than in wild-type PSII preparations. These results are consistent with His332 being close to the Mn cluster and modulating the redox properties of both the Mn cluster and Y_Z. In the present work, we have conducted an ESEEM study of D1-H332E PSII particles to determine if D1-His332 ligates the Mn cluster. We find that the histidine nitrogen modulation observed near 5 MHz in ESEEM spectra of the S_2 state multiline EPR signal of wild-type PSII particles is substantially diminished in D1-H332E PSII particles, consistent with ligation of the Mn cluster by D1-His332. However, alternate explanations are possible.

MATERIALS AND METHODS

Construction of Site-Directed Mutants. The D1-H332E mutation was constructed in the *psbA-2* gene of the cyanobacterium *Synechocystis* sp. strain PCC 6803 (*56*). The plasmid bearing this mutation was transformed into a host strain of *Synechocystis* that lacks all three *psbA* genes (*59*) and contains a hexahistidine-tag (His-tag) fused to the *C*-terminus of CP47 (see next paragraph). Single colonies were selected for ability to grow on solid media containing 5 μg/mL kanamycin monosulfate (*59*). The control wild-type* strain was constructed in identical fashion as the D1-H332E mutant except that the transforming plasmid carried no site-directed mutation. The designation "wild-type*" differentiates this strain from the native wild-type strain that contains all three *psbA* genes and is sensitive to antibiotics.

Construction of Synechocystis Host Strain Containing a His-tag on the C-Terminus of CP47. A 1034 bp fragment of *Synechocystis* genomic DNA containing 341 bp of *psbB* plus downstream flanking DNA was obtained from a plasmid bearing a 5.7 kb *Bam*HI/*Bam*HI fragment containing most of the *psbB* gene (*60*) (a kind gift from W. F. J. Vermaas, Arizona State University). The 1034 bp fragment was cloned into pUC119 (*61*) to generate the plasmid pCP47. A hexahistidine-tag construct containing six histidine codons inserted before the TAG stop codon of *psbB*, $(CACCAT)_2$-$(CAC)_2$TAG (*62*), was obtained by overlap extension PCR (*63*−*65*) of pCP47. The 86 bp *Bst*EII/*Bst*EII fragment of pCP47, containing the TAG stop codon, was then replaced by the 104 bp *Bst*EII/*Bst*EII fragment of the PCR-amplified construct containing the hexahistidine-tag. Finally, a 1.9 kb fragment of the plasmid pRZ1107 (*66*), conferring resistance to gentamycin (Gm^r), was inserted into the *Mfe*I site located 319 bp downstream of the TAG stop codon and 52 bp upstream of the unidentified open region frame, slr0907 (*67*). The final plasmid, pCP47His-tagGm^r, was transformed into cells of the *Synechocystis* host strain lacking all three *psbA* genes (*59*), and single colonies were selected for ability to grow on solid media containing 20 μg/mL gentamycin sulfate. After segregation, homozygous Gm^r transformants containing the His-tag construct were identified by the loss of the *Avr*II site located at the TAG codon in digests of PCR-amplified genomic DNA and by DNA sequence analysis of PCR-amplified genomic DNA.

Propagation of Cultures. Wild-type* and D1-H332E cells were maintained on solid BG-11 media (*68*) containing 5 mM TES−NaOH (pH 8.0), 0.3% (w/v) sodium thiosulfate, 5 mM glucose, 10 μM DCMU, and 5 μg/mL kanamycin monosulfate, as described previously (*50*). The DCMU,

kanamycin monosulfate, and sodium thiosulfate were omitted from liquid cultures. For isolation of PSII particles, cells were grown in modified 250 mL Erlenmeyer flasks as described previously (*50*) until they reached an optical density of 0.9−1.2 at 730 nm. Cells were then transferred to two 20 L carboys, each containing 15 L of growth medium, and grown as described previously (*69*) until their optical densities reached 0.9−1.2 at 730 nm (typically 4 days for wild-type* and 6 days for D1-H332E cells). Optical densities were measured with a CARY 219 spectrophotometer.

Isolation of Synechocystis PSII Particles. All operations following cell harvesting were conducted under dim green light. Thylakoid membranes were isolated (40−100 mg of Chl from 30 L of cells) and extracted with *n*-dodecyl *β*-D-maltoside (Anatrace Inc., Maumee, OH) as described by Tang and Diner (*70*) with minor modification (*69*). The soluble *n*-dodecyl *β*-D-maltoside extract was mixed with 40 mL of Ni−NTA superflow affinity resin (Qiagen Inc., Valencia, CA) that had been equilibrated with sample buffer [25% (v/v) glycerol, 50 mM MES−NaOH (pH 6.0), 20 mM $CaCl_2$, 5 mM $MgCl_2$, 0.03% (w/v) *n*-dodecyl *β*-D-maltoside] in a 5 cm diameter chromatography column. The column was stoppered and placed on a nutatory platform for 30 min of gentle agitation in darkness [longer times (e.g., 1 h) proved deleterious]. The column was then allowed to pack by gravity, and the resin was washed with 10−20 volumes of sample buffer to remove PSI and other contaminants. Purified PSII particles were eluted in 7−10 column volumes with sample buffer containing 25 mM histidine [elution with high concentrations of imidazole (e.g., 250 mM) proved deleterious]. The eluent was brought to 1 mM EDTA, concentrated by ultrafiltration (Amicon models 2000 and 8400 fitted with YM-100 membranes) to a volume of 5−10 mL, brought to 6 mM EDTA, passed through a G-25 column to remove histidine, EDTA, and EDTA-complexed metal ions, then concentrated to 1−2 mg of Chl/mL (Amicon models 8050 and 8010 fitted with YM-100 membranes), frozen in liquid N_2, and stored at −80 °C. For EPR and ESEEM experiments, PSII particles were further concentrated to 4−8 mg of Chl/mL with Centricon-100 concentrators (Millipore Corp., Bedford, MA), mixed with DCMU dissolved in DMSO [to 1 mM DCMU and 1% (v/v) DMSO], loaded into 3.8 mm o.d. precision quartz EPR tubes, dark-adapted 20−30 min on ice, and then frozen in liquid N_2. The O_2 evolution activity of the wild-type* PSII particles was 2.8−4.0 mmol of O_2 (mg of Chl)$^{-1}$ h^{-1}. Data obtained with four separate D1-H332E PSII particle preparations (#1−#4) are reported.

Isolation of Spinach PSII Membranes and Core Particles. All operations were conducted under dim green light. Spinach PSII membranes were purified as described by Berthold et al. (*71*) and Ford and Evans (*72*), with the modifications described previously (*73*). Spinach PSII core particles were isolated from PSII membranes by solubilization with 1-octyl *β*-D-glucopyranoside as described by Ghanotakis et al. (*74*), with the modifications described previously (*73*). Spinach samples were concentrated by centrifugation. The pellets (11−20 mg of Chl/mL) were loaded into 3.8 mm o. d. precision quartz EPR tubes and were frozen immediately in liquid N_2.

EPR, ESE, and ESEEM Measurements. Continuous-wave EPR spectra were recorded with a Bruker ECS106 X-band CW-EPR spectrometer equipped with an ER-4116DM dual mode cavity. Cryogenic temperatures were obtained with an Oxford ESR900 liquid helium cryostat. The temperature was controlled with an Oxford ITC503 temperature and gas flow controller that was equipped with a gold−iron chromel thermocouple. Field-swept two-pulse ESE spectra and two-pulse ESEEM spectra were recorded with a laboratory-built pulsed EPR spectrometer (*75*). For each sample, both the background field-swept two-pulse ESE spectrum and the background two-pulse time domain ESEEM patterns were obtained before the sample was illuminated. To isolate the ESEEM patterns of the S_2 state multiline EPR signal, the ESEEM patterns obtained prior to illumination were subtracted from the ESEEM patterns obtained after illumination. The light-*minus*-dark ESEEM patterns were normalized to their first maximum so that the calculated frequency domain ESEEM spectra would correspond to normalized multiline signal intensities. Frequency domain ESEEM spectra were obtained by calculating the cosine Fourier transforms of the normalized light-*minus*-dark two-pulse time domain data after reconstruction of the instrumental dead times with the Fourier backfill method described by Mims (*76*). Frequencies used for Fourier backfilling were adjusted to the measured frequencies of each Fourier transform and are included in the legend to Figure 5. The same relative amplitudes were used for each class of backfilled frequency components to allow for a quantitative comparison of the final Fourier transforms. Nitrogen modulation at 4.4−4.8 MHz was included in all backfills to avoid any possible bias against, and to obtain an upper limit for, nitrogen modulation in the D1-H332E samples. To generate the S_2 state in *Synechocystis* preparations, samples (containing DCMU) were illuminated in a non-silvered dewar at 273 K (ice/water) for 1 min with a focused 300 W IR-filtered Radiac light source and a Schott 150 W IR-filtered fiber optic lamp. The samples were immediately frozen in an isopentane/liquid N_2 slurry [∼113 K (*77*)], equilibrated in this bath for 30 s, and then transferred to liquid N_2. These conditions were chosen because of the approximately 100 K higher threshold for forming the S_2 state in D1-H332E PSII particles than in wild-type PSII preparations (*58*). To generate the S_2 state in spinach preparations, samples were either illuminated as described for *Synechocystis* preparations (after the addition of DCMU) or illuminated in a non-silvered dewar at 195 K (methanol/dry ice) for 5 min with the Radiac light source and then transferred to liquid N_2. The illumination method employed for each spinach sample is noted in the text and figure legends.

Other Procedures. Chlorophyll concentrations and light-saturated rates of oxygen evolution were measured as described previously for *Synechocystis* (*50*, *69*) and spinach (*73*) PSII preparations.

RESULTS

We have long sought to employ ESEEM spectroscopy to determine if D1-His332 ligates the Mn cluster in PSII. Unfortunately, D1-H332E PSII particles purified by conventional methods incorporating ion-exchange chromatography (*58*) proved unsuitable for these studies because the Mn cluster appeared to be insufficiently stable: Mn^{2+} ions released during sample preparation frustrated all attempts to acquire reliable ESEEM data. Attempts to stabilize the Mn

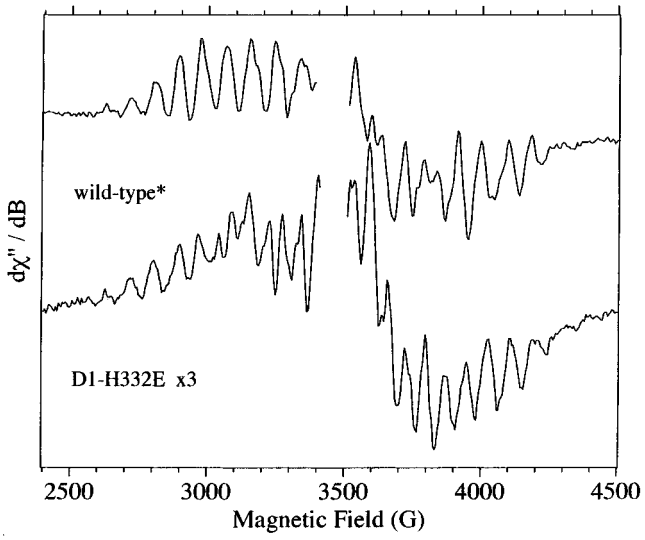

FIGURE 1: Light-*minus*-dark EPR spectrum of wild-type* (upper trace) and D1-H332E (lower trace) PSII particles. Both spectra have the large signal of $Y_D^{\bullet}$ at $g = 2$ excised for clarity. To facilitate comparison of spectra, the amplitude of the D1-H332E spectrum has been multiplied by a factor of 3. The samples were illuminated for 1 min at 273 K before being flash-frozen in an isopentane/liquid N_2 bath (~113 K). The wild-type* and D1-H332E samples contained 7.3 and 7.2 mg of Chl/mL, respectively, in 25% (v/v) glycerol, 50 mM MES−NaOH (pH 6.0), 20 mM $CaCl_2$, 5 mM $MgCl_2$, 0.03% (w/v) *n*-dodecyl-*β*-D-maltoside, 1 mM DCMU, 1% (v/v) DMSO. Experimental conditions: microwave frequency, 9.67 GHz; microwave power, 5 mW; modulation amplitude, 10 G; modulation frequency, 100 kHz; time constant, 41 ms; conversion time, 82 ms; temperature, 7 K. The wild-type* and D1-H332E spectra represent the averages of 32 and 48 scans, respectively.

cluster during isolation of D1-H332E PSII particles or to remove released Mn^{2+} ions were not successful. However, after the successful fusion of a hexahistidine-tag to the *C*-terminus of CP47 in wild-type cells of *Synechocystis* sp. strain PCC 6803 by Brudvig, Diner, and co-workers (*62*) and by Bricker and co-workers (*78*), we set out to fuse a hexahistidine-tag to the *C*-terminus of CP47 in our *Synechocystis* host strain that lacks all three *psbA* genes (*59*). The His-tag permits PSII particles to be purified with metal affinity chromatography. Utilization of metal affinity chromatography permits purification to be carried out at substantially lower ionic strengths than are required in conventional purification schemes employing ion exchange chromatography. The lower ionic strengths presumably preserve the intactness of the Mn cluster by avoiding dissociation of the extrinsic proteins that stabilize the cluster. In addition to providing PSII particles with more stable Mn clusters, the His-tag method provides PSII particles that are considerably purer and provides them in greater yields (2−3-fold) than previously possible.

Continuous-Wave EPR Spectra. As reported previously (*58*), the S_2 state multiline EPR signal of D1-H332E PSII particles, obtained after illumination at 273 K in the presence of DCMU, has more hyperfine lines and narrower splittings than the S_2 state multiline EPR signal of wild-type* PSII particles (Figure 1). The signal of D1-H332E PSII particles superficially resembles the signals of native spinach and cyanobacterial PSII preparations treated with ammonia (*79*−*81*) or having Ca replaced with Sr (*81*, *82*). The S_1 state multiline EPR signal observed in His-tagged wild-type* PSII particles (not shown) and the S_2 state multiline EPR signals observed in both His-tagged wild-type* and D1-H332E PSII particles (Figure 1) are the same as those observed in PSII particles purified by conventional methods (*58*, *83*), confirming that the presence of the His-tag on CP47 does not alter the properties of the Mn cluster in *Synechocystis* sp. strain PCC 6803 (*62*, *78*, *84*, *85*). Similarly, the presence of a His-tag on the *C*-terminus of CP43 does not alter the properties of the Mn cluster in *Synechococcus elongatus* (*86*, *87*).

ESE Field-Swept EPR Spectra. The ESE field-swept EPR spectra of *Synechocystis* wild-type* and D1-H332E PSII particles are compared to those of spinach PSII membranes and core particles in Figure 2. The spectrum of spinach PSII core particles (Figure 2B) resembles that of spinach PSII membranes (Figure 2A), except that the latter has a larger background signal in dark-adapted samples (approximately 3-fold larger on a reaction center basis), and both are similar to ESE field-swept EPR spectra of spinach PSII membranes that have been published previously (*11*, *30*, *32*, *88*). The spectra of *Synechocystis* wild-type* and D1-H332E PSII particles (Figures 2C and 2D, respectively) resemble each other and are similar to the ESE field-swept EPR spectrum of *Synechocystis* wild-type* PSII particles reported previously (*43*). The background signals in dark-adapted *Synechocystis* preparations resemble those of spinach PSII core particles. The light-*minus*-dark S_2 state spectra of the *Synechocystis* preparations resemble those of spinach PSII membranes and core particles. Illumination of some *Synechocystis* PSII preparations (primarily those agitated for 1 h with Ni−NTA resin or eluted with 250 mM imidazole) caused a significant decrease of the peak near 2300 G (not shown). This peak corresponds to the g_z turning point of the oxidized form of cytochrome *b*-559. The peak's decrease is evidence of an apparent photoreduction of this cytochrome. The EPR signal of the oxidized form of cytochrome *b*-559 underlies much of the S_2 state multiline EPR signal [$g_z \approx 3.0$, $g_y \approx 2.2$, and $g_x \approx 1.5$ for cytochrome *b*-559 in *Synechocystis* sp. strain PCC 6803 (*89*)]. Furthermore, the frequency domain ESEEM spectrum of cytochrome *b*-559 exhibits peaks near 4, 7.2, and 11.4 MHz (*90*). Therefore, any photoreduction of cytochrome *b*-559 could contaminate the S_2 state ESEEM spectra with subtraction artifacts from the cytochrome heme and histidyl ligand nitrogens. Consequently, data from *Synechocystis* wild-type* and D1-H332E samples in which substantial photoreduction of cytochrome *b*-559 was observed were not included in our analysis of histidyl ligation in the D1-H332E mutant. That the photoreduced cytochrome is cytochrome *b*-559 and not cytochrome *c*-550, an extrinsic subunit of PSII in cyanobacteria (*6*, *91*), is suggested by our observation of apparent cytochrome photoreduction in some preparations of spinach PSII core particles (e.g., Figure 2B). The reduction of cytochrome *b*-559 by $Q_A^{\bullet -}$ (*92*) or by $Pheo^{\bullet -}$ [either directly (*93*−*96*) or indirectly (*97*)] has been proposed, but the mechanism of photoreduction is unknown.

The light-induced S_2 state multiline signals observed in *Synechocystis* wild-type* and D1-H332E PSII particles are significantly smaller than those observed in spinach PSII preparations on a reaction center basis, whether measured with ESE spectroscopy (Figure 2) or with continuous-wave EPR spectroscopy (not shown). Assuming 250 Chl/PSII in spinach PSII membranes (*71*), 70 Chl/PSII in spinach PSII core preparations (*74*, *98*), and 38 Chl/PSII in *Synechocystis*

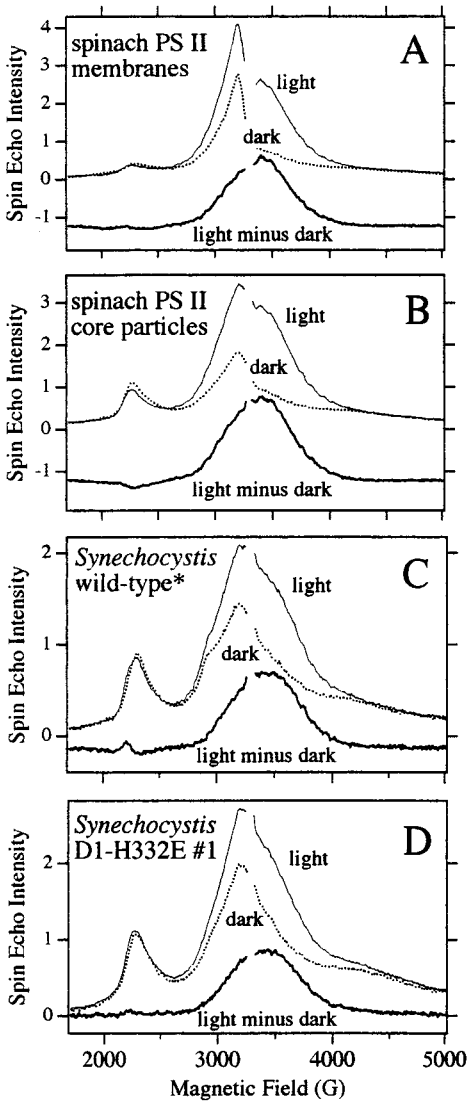

FIGURE 2: ESE field-swept EPR spectra of (A) spinach PSII membranes, (B) spinach PSII core particles, (C) *Synechocystis* wild-type* PSII particles, and (D) *Synechocystis* D1-H332E PSII particles (from preparation #1). Each panel shows the ESE field-swept EPR spectrum of the sample prior to illumination (middle traces), the ESE field-swept EPR spectrum of the sample after illumination (upper traces), and the light-*minus*-dark difference spectrum (lower traces). In panels A−C, the light-*minus*-dark difference spectra have been offset for clarity. All spectra have the large signal of $Y_D^\bullet$ at $g = 2$ excised for clarity. The spinach samples were illuminated for 5 min at 200 K (methanol/dry ice). The *Synechocystis* samples were illuminated for 1 min at 273 K (ice water) before being flash-frozen in an isopentane/liquid N_2 bath (∼113 K). The samples contained 18, 11, 6.5, and 4.2 mg of Chl/mL, respectively. The spinach PSII membranes were in 0.4 M sucrose, 50 mM MES−NaOH (pH 6.0), 15 mM NaCl, 5 mM $MgCl_2$, 5 mM $CaCl_2$, and 1 mM EDTA. The spinach PSII core particles were in 0.4 M sucrose, 50 mM MES−NaOH (pH 6.0), 10 mM NaCl, and 5 mM $CaCl_2$. The *Synechocystis* wild-type* and D1-H332E PSII particles were in 25% (v/v) glycerol, 50 mM MES−NaOH (pH 6.0), 20 mM $CaCl_2$, 5 mM $MgCl_2$, 0.03% (w/v) *n*-dodecyl-*β*-D-maltoside, 1 mM DCMU, 1% (v/v) DMSO. Experimental conditions: microwave frequency, 9.221 GHz; microwave pulse peak power, 22 W; $\pi/2$ pulse width, 15 ns; π pulse width, 25 ns; τ, 210 ns; repetition time, 5 ms; temperature, 4.2 K.

PSII particles (*70*), the amplitudes of the light-*minus*-dark S_2 state ESE field-swept EPR spectra were approximately 4-fold smaller in *Synechocystis* wild-type* PSII particles than in spinach PSII membranes. The origin of this smaller multiline amplitude needs to be further investigated. Perhaps a larger fraction of *Synechocystis* S_2 state PSII particles are partitioned into conformations not giving rise to the S_2 state multiline EPR signal, such as the spin ≥ 5/2 state conformation that shows EPR signals at $g > 5$ (*99*, *100*). This spin state conformation has been shown to be more stable in *Synechococcus elongatus* than in spinach (*100*). Nevertheless, when normalized to their maximum amplitudes, the light-*minus*-dark ESE field-swept EPR spectra of the S_2 state multiline signal in wild-type* and D1-H332E *Synechocystis* PSII particles closely resemble those obtained with spinach PSII membranes and core particles in terms of width and overall line shape (Figure 3).

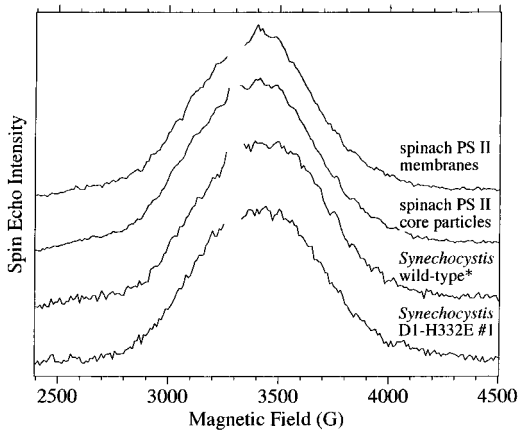

FIGURE 3: Normalized light-*minus*-dark ESE field-swept EPR spectra of spinach PSII membranes, spinach PSII core particles, *Synechocystis* wild-type* PSII particles, and *Synechocystis* D1-H332E PSII particles (from preparation #1). Data and parameters from Figure 2.

ESEEM Spectra. Two-pulse time domain ESEEM patterns recorded at a consistent magnetic field position (3415 G) where the light-*minus*-dark ESE field-swept EPR spectra were near-maximal in all samples are shown in Figure 4 for spinach PSII membranes, spinach PSII core particles, *Synechocystis* wild-type* PSII particles, and *Synechocystis* D1-H332E PSII particles. To isolate the modulations from coupled magnetic nuclei to only the S_2 state of the Mn cluster, the background ESEEM patterns were subtracted from the light-induced ESEEM patterns to yield the light-*minus*-dark ESEEM patterns shown in boldface. Frequency domain ESEEM spectra were calculated from the normalized light-*minus*-dark time domain patterns after reconstruction of the instrumental dead times (Figure 5). These Fourier transform spectra are shown evenly shifted in a cascade plot having a constant amplitude scale so that peak amplitudes can be compared directly. To avoid any possible bias against nitrogen modulation in the frequency domain ESEEM spectra of the D1-H332E samples, nitrogen modulation at 4.4−4.8 MHz was included in the backfills of *all* samples (the exact parameters used for each sample are listed in the legend to Figure 5). As a comparison, backfills were also calculated for all samples *without* these nitrogen modulation parameters. The effect of omitting the nitrogen modulation parameters increased the amplitude of the proton peaks at ∼15 MHz by 1.4 ± 0.3% and decreased the amplitude of the nitrogen peaks by 17 ± 2% in all samples (not shown). Our conclusions are the same with either backfilling method. Therefore, we have chosen to display the frequency domain ESEEM spectra obtained by including nitrogen modulation

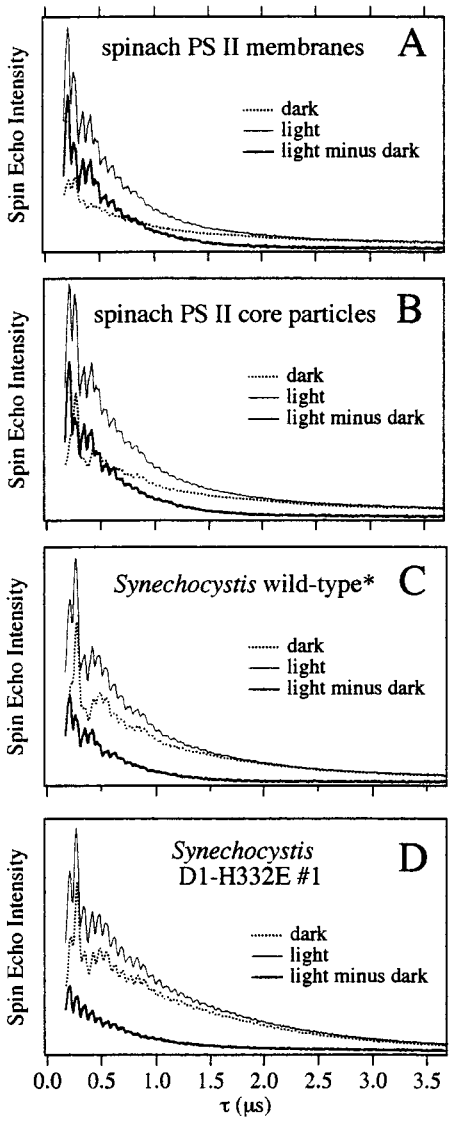

FIGURE 4: Two-pulse time-domain ESEEM patterns of (A) spinach PSII membranes, (B) spinach PSII core particles, (C) *Synechocystis* wild-type* PSII particles, and (D) *Synechocystis* D1-H332E PSII particles (from preparation #1). Shown are the ESEEM patterns of the samples prior to illumination (dotted lines), the ESEEM patterns after illumination (sold lines), and their difference (boldface lines), corresponding to the ESEEM patterns of the light-induced S_2 state of the Mn cluster. The samples are those used in Figures 2 and 3. Experimental conditions: magnetic field, 3415 G; microwave frequency, 9.221 GHz; $\pi/2$ pulse width, 15 ns; π pulse width, 25 ns; repetition time, 5 ms; microwave pulse peak power, 22 W; temperature, 4.2 K. The interval, τ, between pulses in the two-pulse sequence was increased from 170 to 3670 ns in 10 ns increments.

in all backfills to obtain an upper limit for nitrogen modulation in the D1-H332E samples.

Frequency domain ESEEM spectra of spinach PSII membranes are shown at the top of Figure 5. The solid line corresponds to the sample shown in Figures 2A and 4A. This sample was illuminated at 195 K. The dashed line corresponds to a different preparation of PSII membranes that contained DCMU and was illuminated for 1 min at 273 K. These data show that the two illumination conditions are essentially equivalent for spinach PSII preparations. The frequency domain ESEEM spectra of two different preparations of spinach PSII core particles are also shown near the

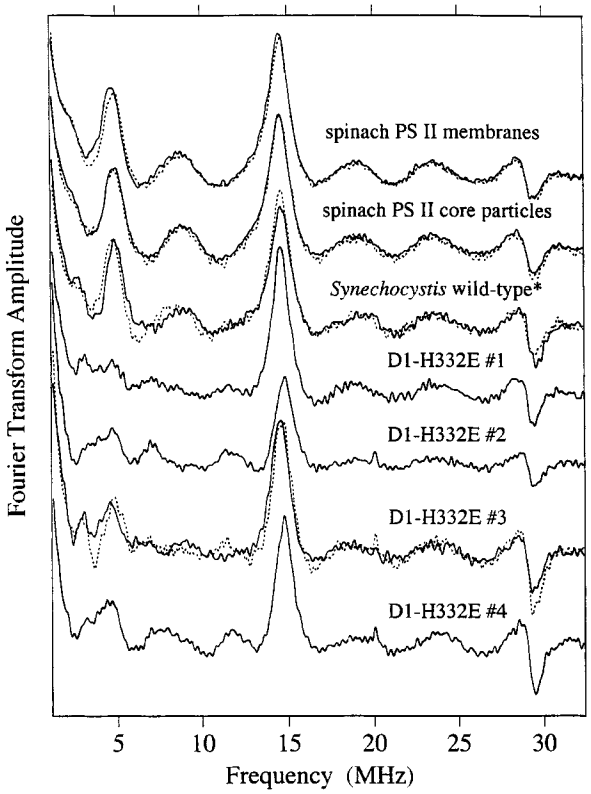

FIGURE 5: Cosine Fourier transforms of normalized two-pulse time domain light-*minus*-dark ESEEM patterns of spinach PSII membranes, spinach PSII core particles, *Synechocystis* wild-type* PSII particles, and four independent preparations of *Synechocystis* D1-H332E PSII particles (preparations #1−#4) calculated after reconstruction of the instrumental dead times (0−170 ns). Spectra are shown evenly shifted in a cascade plot having a constant amplitude scale, so that peak amplitudes can be compared directly. For the spinach and *Synechocystis* wild-type* transforms, the solid lines correspond to the samples shown in Figures 2−4. For the spinach PSII membranes, the solid and dashed lines correspond to independent preparations that were illuminated at 195 and 273 K, respectively. For the spinach PSII core and *Synechocystis* wild-type* PSII particles, the solid and dashed lines correspond to independent sample preparations. Both of the spinach PSII core preparations were illuminated at 195 K. All of the *Synechocystis* wild-type* and D1-H332E PSII preparations were illuminated for 1 min at 273 K. For D1-H332E PSII preparation #3, the dashed line corresponds to an independent aliquot of the same sample. Sample concentrations: 18 and 20 mg of Chl/mL for spinach PSII membranes (solid and dashed lines, respectively); 11 and 20 mg of Chl/mL for spinach PSII core particles (solid and dashed lines, respectively); 6.5 and 4.7 mg of Chl/mL for *Synechocystis* wild-type* PSII particles (solid and dashed lines, respectively); 4.2, 5.9, 5.9, and 8.2 mg of Chl/mL for *Synechocystis* D1-H332E PSII particle preparations #1, #2, #3, and #4, respectively. Experimental conditions: same as Figure 4 except for three samples (the *Synechocystis* wild-type* preparation shown with a dashed line and D1-H332E preparations #2 and #3) for which the magnetic field was 3420 G and the microwave frequency was 9.235 GHz. Relative amplitudes of frequency components (0.4 MHz width each) used in Fourier backfilling to reconstruct the instrumental dead times: 3 (4.4−4.8 MHz), 20 (14.5−14.7 MHz), and 10 (29.3−29.5 MHz). Specific frequencies used in backfills: for nitrogen, 4.4 MHz in D1-H332E #4, 4.5 MHz in D1-H332E #3 (solid), 4.6 MHz in spinach PSII membranes (solid), *Synechocystis* wild-type* (solid), D1-H332E #1, D1-H332E #2, and D1-H332E #3 (dashed), 4.7 MHz in spinach PSII membranes (dashed), spinach PSII core particles (solid and dashed), and 4.8 MHz in *Synechocystis* wild-type* (dashed); for protons, 14.7 MHz in D1-H332E #2 and #4, 14.5 MHz in all other samples; for proton "sum peak," 29.3 MHz in all D1-H332E samples, 29.5 MHz in *Synechocystis* wild-type* (dashed), and 29.4 MHz in all other samples.

top of Figure 5. Both samples were illuminated at 195 K. The solid line corresponds to the sample shown in Figures 2B and 4B. The dashed line corresponds to an independent preparation and shows the reproducibility of spectra from different preparations of spinach PSII core particles.

The frequency domain ESEEM spectra of two different preparations of *Synechocystis* wild-type* PSII particles are also shown in Figure 5 (all *Synechocystis* PSII preparations were illuminated for 1 min at 273 K). The solid line corresponds to the sample shown in Figures 2C and 4C. The dashed line corresponds to an independent preparation and shows the reproducibility of spectra from different preparations of *Synechocystis* wild-type* PSII particles. Three additional *Synechocystis* wild-type* PSII preparations yielded similar spectra (not shown). It has been suggested that the ligand environment of the Mn cluster in cyanobacteria differs from that in spinach because the spin $\geq 5/2$ state is more rhombic in *Synechococcus elongatus* than in spinach (*100*). However, the similarity of the frequency domain ESEEM spectra of the spinach and *Synechocystis* wild-type* PSII preparations (Figure 5) shows that the environment of the Mn cluster in *Synechocystis* resembles that in spinach, at least in terms of histidyl ligation. Similarity of the coordination environments of the Mn clusters in *Synechocystis* and spinach has also been noted in a recent comparison of mid- and low-frequency S_2-*minus*-S_1 FTIR difference spectra (*85*). The frequency domain ESEEM spectra of four separate D1-H332E PSII preparations (#1−#4) are also shown in Figure 5. The data shown in Figures 2D and 4D were obtained with preparation #1. Two aliquots of D1-H332E preparation #3 are shown in Figure 5 as overlays. To avoid potential artifacts associated with subtracting large background signals, only those *Synechocystis* wild-type* and D1-H332E samples exhibiting the largest light-induced S_2 state multiline EPR signals were included in our analysis (the five wild-type* PSII preparations noted above and the four D1-H332E PSII preparations shown in Figure 5). Similarly, to avoid the possibility of difference ESEEM spectral contamination from cytochrome heme and histidyl nitrogen ligands, only samples exhibiting negligible photoreduction of cytochrome *b*-559 were included in our analysis (the same five wild-type* PSII preparations and the four D1-H332E PSII preparations shown in Figure 5).

In the frequency domain ESEEM spectra of the spinach and *Synechocystis* wild-type* preparations (Figure 5), the peak centered near 5 MHz is similar to that reported previously in spinach (*32*, *88*) and cyanobacterial (*30*, *33*, *43*) PSII preparations and corresponds to nitrogen modulation from one or more Mn histidyl ligands (*33*, *43*). The broad feature near 9 MHz is not reproducible in all wild-type spectra (not shown) and may be an artifact. The peak centered near 15 MHz corresponds to protons that are weakly coupled to the electron spin of the Mn cluster and that are resonating at or near the proton Larmor frequency (*88*). These protons also give rise to the negative "sum" peak that is centered near 29 MHz, at approximately twice the proton Larmor frequency.[2] In all D1-H332E PSII preparations exhibiting large light-induced S_2 state multiline EPR signals and negligible photoreduction of cytochrome *b*-559, the amplitude of the nitrogen modulation at ~5 MHz is substantially diminished compared to that in native PSII preparations from *Synechocystis* and spinach (Figure 5). However, there is significant variance in the actual ESEEM line shapes in the nitrogen region of the D1-H332E preparations.

DISCUSSION

None of the 10 reported mutations constructed at D1-His332 (Gln, Ser, Asn, Asp, Glu, Lys, Arg, Leu, Tyr, and Gly) support photoautotrophic growth (*55*, *56*). Only the D1-H332Q and D1-H332S mutants evolve O_2, but at only 10−15% the rate of wild-type cells (*55*, *56*). In all mutants except D1-H332D and D1-H332E, substantial fractions of PSII complexes lack photooxidizable Mn ions in vivo (*56*), showing that His332 influences the assembly or stability of the Mn cluster. Because Gln and Glu functionally replace His as a ligand to Fe in cytochrome *c* peroxidase (*104*−*106*), and because Asp and Ser are potential ligands to Mn, it was proposed that D1-His332 may ligate the Mn cluster (*56*). The additional hyperfine lines and narrower splittings of the S_2 state multiline EPR signal of intact D1-H332E PSII particles, and the inability of these PSII particles to advance beyond an altered $S_2Y_Z^{\bullet}$ state (*58*), are consistent with D1-His332 being close to the Mn cluster and modulating the redox properties of both the Mn cluster and Y_Z (*58*).

Our results show that the histidyl nitrogen modulation observed near 5 MHz in ESEEM spectra of the S_2 state multiline EPR signal in wild-type* *Synechocystis* PSII particles and spinach PSII preparations is diminished substantially in D1-H332E PSII particles. However, there is significant variance in the ESEEM line shapes in the nitrogen region of the mutant PSII particles, as seen in Figure 5. This variability may represent residual heme nitrogen ligation or subtraction artifacts associated with calculating light-*minus*-dark time domain data despite our inclusion of only D1-H332E PSII particles showing both the largest light-induced S_2 state multiline EPR signals and negligible photoreduction of cytochrome *b*-559. That the ESEEM spectrum of one aliquot of D1-H332E preparation #3 (solid line) resembles more closely the spectrum of preparation #2 than the spectrum of the second aliquot of preparation #3 (dashed line) suggests that subtraction artifacts at least partly explain the variability. Nevertheless, the significantly different line shapes of the four D1-H332E preparations in the nitrogen region suggest that a preparation-dependent heterogeneity may also contribute to the variation. Whatever the origin of this variation, the nitrogen modulation observed near 5 MHz in spinach and *Synechocystis* wild-type* preparations is diminished substantially in all four D1-H332E preparations, as seen in the four individual spectra presented in Figure 5.

We see two explanations for the significantly diminished amplitude of the ~5 MHz histidyl nitrogen modulation in D1-H332E PSII particles. The simplest and most straightforward explanation is that D1-His332 ligates the Mn cluster. The diminished modulation amplitude would then represent either the loss of the ligating D1-His332 $\epsilon 2$ (τ) nitrogen, decreasing the coordination number of one Mn ion from 6 to 5,[3] or the replacement of the ligating nitrogen with an

[2] Density matrix analysis shows that, in addition to the fundamental nuclear spin transition frequencies, the sum and difference of these frequencies also appear in the two-pulse ESEEM spectra; their negative phases result in inverted peaks in the cosine Fourier transform (*101*−*103*).

oxygen from glutamate or with an oxygen from another residue, peptide group, or water molecule (or with some other atom that gives rise to no modulation at 5 MHz). Loss of modulation amplitude at specific frequencies has previously been taken as evidence for the ligation of metal ions by specific histidine residues in the H138S and H143S mutants of phenylalanine hydroxylase (*107*), the H85A mutant of rusticyanin (*108*), and the H117G mutant of azurin (with [^{15}N]imidazole added as an external ligand) (*109*, *110*) [for a review of ESEEM studies of metalloproteins, see (*111*)]. The residual nitrogen modulation in the D1-H332E PSII particles could reflect the presence of a second histidyl ligand in the native protein, with the varying intensity of the residual modulation reflecting preparation-dependent heterogeneities that influence the magnitude of this residue's magnetic coupling near 5 MHz. Alternatively, structural perturbations caused by the replacement of D1-His332's ligating $\epsilon 2$ (τ) nitrogen could cause ligation of the Mn cluster by a previously nonligating nitrogen-containing residue in a preparation-dependent manner.

A second possibility is that D1-His332 does NOT ligate the Mn cluster, but that minor structural perturbations associated with the D1-H332E mutation abolish magnetic couplings between the Mn cluster and the actual histidyl ligand(s), or alter these couplings in such a manner that they are not detectable by ESEEM spectroscopy. Such structural perturbations could be preparation-dependent and involve either the loss/alteration of magnetic couplings from the native histidyl ligands or the replacement of the native histidyl ligands with previously nonligating residues or peptide groups. An example with some relevance is provided by the α-H195N mutation in nitrogenase from *Azotobacter vinelandii*. The ESEEM spectrum of nitrogenase shows deep nitrogen modulation that arises from magnetic coupling between α-Arg359 and the Fe_7Mo cofactor (*114*). This residue forms a hydrogen bond to a sulfide that bridges between Fe and Mo. Several other residues, including α-His195, form single hydrogen bonds to sulfides that bridge between pairs of Fe ions. The α-H195N mutation eliminates the hydrogen bond between α-His195 and one of these sulfide bridges (*114*, *115*). The loss of this hydrogen bond causes the Fe_7Mo cofactor to reorient sufficiently to weaken the hydrogen bond between α-Arg359 and its sulfide, thereby abolishing the magnetic coupling between α-Arg359 and the Fe_7Mo cofactor (*114*, *115*).

Therefore, we cannot exclude the possibility that the altered properties of the D1-H332E mutant only reflect structural perturbations associated with the D1-H332E mutation. One specific possibility is that D1-His332, rather than ligating the Mn cluster, serves in a network of hydrogen bonds that optimizes the configuration of the $(Mn)_4-Y_Z$ complex for rapid electron/proton transfer from the Mn cluster to $Y_Z^{\bullet}$. This possibility has been suggested previously (*56*, *58*). The altered EPR and electron-transfer characteristics (*58*) and the diminished histidyl nitrogen modulation in the ESEEM spectra of D1-H332E PSII particles (Figure 5) might reflect an alteration of this hydrogen bond network caused by replacing the imidazole moiety of D1-His332 with the carboxylate moiety of Glu, resulting in loss/alteration of magnetic couplings from native histidyl ligand(s).[4] In this scenario, D1-His332 would serve as a crucial hydrogen bond donor that can be partly replaced by Gln and by Ser (the latter via an immobilized water molecule). In several systems, Gln functionally replaces His as a hydrogen bond donor. In nitrogenase, the nitrogen modulation that is abolished by the α-H195N mutation is not abolished by the α-H195Q mutation (*115*). In sperm whale myoglobin, His64 provides a crucial hydrogen bond to O_2 that is retained in the H64Q and H64G mutants (the latter via an immobilized water molecule) (*116*). In ribulose-1,5-bisphosphate carboxylase/oxygenase from *Anacystis nidulans*, His324 provides a hydrogen bond to substrate that is retained in the H324Q mutant (*117*). Nevertheless, if the diminished histidyl nitrogen modulation in D1-H332E PSII particles reflects only structural perturbations associated with the mutation, these perturbations must be sufficiently minor to permit the Mn cluster to be assembled and to form an S_2 state. Furthermore, the magnetic properties of this S_2 state are not perturbed to a greater extent than those of the S_2 states in wild-type PSII preparations that have been treated with ammonia (*79*−*81*) or that contain Sr in place of Ca (*81*, *82*).

The analysis of additional D1-His332 mutants by ESEEM spectroscopy should help determine whether the D1-H332E mutation eliminates/replaces a ligating D1-His332 $\epsilon 2$ (τ) nitrogen or merely introduces minor structural perturbations that diminish or abolish the magnetic couplings between another histidyl ligand and the electron spin of the Mn cluster. One such mutant is D1-H332Q. Because D1-H332Q cells evolve O_2, whereas D1-H332E cells do not (*56*), perturbations associated with the D1-H332Q mutation may be fewer than those possibly associated with the D1-H332E mutation. In cytochrome *c* peroxidase, Gln replaces His175

[3] It is intriguing to speculate that the altered line shape of the S_2 state multiline EPR signal of D1-H332E PSII particles correlates with a decrease in the coordination number of a Mn(III) ion. Converting a six-coordinate Mn(III) ion from a conventional tetragonally elongated octahedral geometry to a five-coordinate trigonal bipyramidal geometry [such as found for the Mn(III) ion in Mn superoxide dismutase (*112*)] would reverse the sign of the dipolar component of the hyperfine tensor (*11*, *113*). Interestingly, such a reversal in sign emerged from a recent EPR/ENDOR spectral simulation of the altered S_2 state multiline EPR signal in ammonia-treated PSII preparations (*11*). The altered line shape of the ammonia-modified signal (*79*−*81*) superficially resembles the line shape of the signal in D1-H332E PSII particles. Perhaps a reduction of coordination number in the D1-His332 mutant leads to a dipolar coupling sign reversal in a fashion directly analogous to what was modeled for the ammonia-altered signal.

[4] Note that we are not suggesting that the histidyl nitrogen modulation in wild-type PSII preparations corresponds to D1-His332 coupled to the Mn cluster through a hydrogen bond. The strength of this modulation is more consistent with direct coordination of Mn by histidyl nitrogens (*33*, *43*). Multifrequency ESEEM simulations (*43*) suggest that the ^{14}N histidine hyperfine couplings for the S_2 state are as least as strong as those observed for a variety of directly coordinating ^{14}N ligands over a range of Mn(III)Mn(IV) dinuclear complexes (*118*, *119*). We do not have comparable data on tetranuclear Mn model compounds which might serve as better spectral models for the S_2 state multiline signal. However, our recent ^{55}Mn ENDOR study (*11*) shows that the quantum mechanical projection factors determining the hyperfine interactions of the four Mn ions of the S_2 state PSII cluster are roughly equivalent to those of the Mn(IV) ion of such Mn(III)Mn(IV) dinuclear clusters, and only approximately half that of the Mn(III) ion. Given this observation, one would expect comparable, or perhaps weaker, hyperfine interactions with ligands of the S_2 state Mn cluster in PSII. Because the current spectra simulations use comparably strong ^{14}N hyperfine couplings for the S_2 state histidine(s) as for the ligated nitrogens of the dinuclear models, we favor direct histidine coordination to the Mn cluster in PSII.

as a ligand to heme and is believed to ligate the Fe with its oxygen atom (*104*).

CONCLUDING REMARKS

The histidyl nitrogen modulation observed near 5 MHz in ESEEM spectra of the S_2 state multiline EPR signal in native PSII preparations is substantially diminished in D1-H332E PSII particles. This result is consistent with ligation of the Mn cluster by D1-His332, but could also be caused by a structural perturbation induced by the D1-H332E mutation. Distinguishing between these and other possibilities will require ESEEM studies of additional D1-His332 mutants.

ACKNOWLEDGMENT

We are grateful to M. J. Reifler for advice on preparing the His-tag construct, to M. J. Reifler, D. A. Force, and T. M. Bricker for advice on purifying *Synechocystis* PSII particles by metal affinity chromatography, and to A. P. Nguyen for isolating the thylakoid membranes and for maintaining the wild-type* and mutant cultures of *Synechocystis* 6803.

REFERENCES

1. Debus, R. J. (1992) *Biochim. Biophys. Acta 1102*, 269−352.
2. Britt, R. D. (1996) in *Oxygenic Photosynthesis: The Light Reactions* (Ort, D. R., and Yocum, C. F., Eds.) pp 137−164, Kluwer Academic Publishers, Dordrecht, The Netherlands.
3. Yachandra, V. K., Sauer, K., and Klein, M. P. (1996) *Chem. Rev. 96*, 2927−2950.
4. Penner-Hahn, J. E. (1998) *Struct. Bonding 90*, 1−36.
5. Hoganson, C. W., and Babcock, G. T. (2000) *Met. Ions Biol. Syst. 37*, 613−656.
6. Debus, R. J. (2000) *Met. Ions Biol. Syst. 37*, 657−711.
7. Pecoraro, V. L., and Hsieh, W.-Y. (2000) *Met. Ions Biol. Syst. 37*, 429−504.
8. Tommos, C., and Babcock, G. T. (2000) *Biochim. Biophys. Acta 1458*, 199−219.
9. Renger, G. (2001) *Biochim. Biophys. Acta 1503*, 210−228.
10. Randall, D. W., Sturgeon, B. E., Ball, J. A., Lorigan, G. A., Chan, M. K., Klein, M. P., Armstrong, W. H., and Britt, R. D. (1995) *J. Am. Chem. Soc. 117*, 11780−11789.
11. Peloquin, J. M., Campbell, K. A., Randall, D. W., Evanchik, M. A., Pecoraro, V. L., Armstrong, W. H., and Britt, R. D. (2000) *J. Am. Chem. Soc. 122*, 10926−10942.
12. Britt, R. D., Peloquin, J. M., and Campbell, K. A. (2000) *Annu. Rev. Biophys. Biomol. Struct. 29*, 463−495.
13. Peloquin, J. M., and Britt, R. D. (2001) *Biochim. Biophys. Acta 1503*, 96−111.
14. Zouni, A., Witt, H. T., Kern, J., Fromme, P., Krauss, N., Saenger, W., and Orth, P. (2001) *Nature 409*, 739−743.
15. Robblee, J. H., Cinco, R. M., and Yachandra, V. K. (2001) *Biochim. Biophys. Acta 1503*, 7−23.
16. Dau, H., Iuzzolino, L., and Dittmer, J. (2001) *Biochim. Biophys. Acta 1503*, 24−39.
17. Boussac, A., Zimmermann, J.-L., Rutherford, A. W., and Lavergne, J. (1990) *Nature 347*, 303−306.
18. MacLachlan, D. J., Nugent, J. H. A., Warden, J. T., and Evans, M. C. W. (1994) *Biochim. Biophys. Acta 1188*, 325−334.
19. Peloquin, J. M., Campbell, K. A., and Britt, R. D. (1998) *J. Am. Chem. Soc. 120*, 6840−6841.
20. Dorlet, P., Di Valentin, M., Babcock, G. T., and McCracken, J. L. (1998) *J. Phys. Chem. B 102*, 8239−8247.
21. Lakshmi, K. V., Eaton, S. S., Eaton, G. R., Frank, H. A., and Brudvig, G. W. (1998) *J. Phys. Chem. B 102*, 8327−8335.
22. Lakshmi, K. V., Eaton, S. S., Eaton, G. R., and Brudvig, G. W. (1999) *Biochemistry 38*, 12758−12767.
23. Dorlet, P., Boussac, A., Rutherford, A. W., and Un, S. (1999) *J. Phys. Chem. B 103*, 10945−10954.
24. Tommos, C., and Babcock, G. T. (1998) *Acc. Chem. Res. 31*, 18−25.
25. Limburg, J., Szalai, V. A., and Brudvig, G. W. (1999) *J. Chem. Soc., Dalton Trans.*, 1353−1361.
26. Westphal, K. L., Tommos, C., Cukier, R. I., and Babcock, G. T. (2000) *Curr. Opin. Plant Biol. 3*, 236−242.
27. Vrettos, J. S., Limburg, J., and Brudvig, G. W. (2001) *Biochim. Biophys. Acta 1503*, 229−245.
28. Diner, B. A. (2001) *Biochim. Biophys. Acta 1503*, 147−163.
29. Debus, R. J. (2001) *Biochim. Biophys. Acta 1503*, 164−186.
30. DeRose, V. J., Yachandra, V. K., McDermott, A. E., Britt, R. D., Sauer, K., and Klein, M. P. (1991) *Biochemistry 30*, 1335−1341.
31. Tang, X.-S., Sivaraja, M., and Dismukes, G. C. (1993) *J. Am. Chem. Soc. 115*, 2382−2389.
32. Zimmermann, J.-L., Boussac, A., and Rutherford, A. W. (1993) *Biochemistry 32*, 4831−4841.
33. Tang, X.-S., Diner, B. A., Larsen, B. S., Gilchrist, M. L., Jr., Lorigan, G. A., and Britt, R. D. (1994) *Proc. Natl. Acad. Sci. U.S.A. 91*, 704−708.
34. Tamura, N., Ikeuchi, M., and Inoue, Y. (1989) *Biochim. Biophys. Acta 973*, 281−289.
35. Seibert, M., Tamura, N., and Inoue, Y. (1989) *Biochim. Biophys. Acta 974*, 185−191.
36. Preston, C., and Seibert, M. (1991) *Biochemistry 30*, 9615−9624.
37. Preston, C., and Seibert, M. (1991) *Biochemistry 30*, 9625−9633.
38. Blubaugh, D. J., and Cheniae, G. M. (1992) in *Research in Photosynthesis* (Murata, N., Ed.) Vol. II, pp 361−364, Kluwer Academic Publishers, Dordrecht, The Netherlands.
39. Magnuson, A., and Andréasson, L.-E. (1997) *Biochemistry 36*, 3254−3261.
40. Tamura, N., Noda, K., Wakamatsu, K., Kamachi, H., Inoue, H., and Wada, K. (1997) *Plant Cell Physiol. 38*, 578−585.
41. Ghirardi, M. L., Lutton, T. W., and Seibert, M. (1998) *Biochemistry 37*, 13559−13566.
42. Ghirardi, M. L., Preston, C., and Seibert, M. (1998) *Biochemistry 37*, 13567−13574.
43. Gilchrist, M. L., Jr. (1996) Ph.D. Dissertation, University of California, Davis, CA.
44. Noguchi, T., Inoue, Y., and Tang, X.-S. (1999) *Biochemistry 38*, 10187−10195.
45. Noguchi, T., Ono, T.-A., and Inoue, Y. (1995) *Biochim. Biophys. Acta 1228*, 189−200.
46. Smith, J. C., Gonzalez-Vergara, E., and Vincent, J. B. (1997) *Inorg. Chim. Acta 255*, 99−103.
47. Chu, H.-A., Hillier, W., Law, N. A., and Babcock, G. T. (2001) *Biochim. Biophys. Acta 1503*, 69−82.
48. Nixon, P. J., and Diner, B. A. (1992) *Biochemistry 31*, 942−948.
49. Boerner, R. J., Nguyen, A. P., Barry, B. A., and Debus, R. J. (1992) *Biochemistry 31*, 6660−6672.
50. Chu, H.-A., Nguyen, A. P., and Debus, R. J. (1994) *Biochemistry 33*, 6137−6149.
51. Whitelegge, J. P., Koo, D., Diner, B. A., Domian, I., and Erickson, J. M. (1995) *J. Biol. Chem. 270*, 225−235.
52. Chu, H.-A., Nguyen, A. P., and Debus, R. J. (1995) *Biochemistry 34*, 5839−5858.
53. Nixon, P. J., Chisholm, D. A., and Diner, B. A. (1992) in *Plant Protein Engineering* (Shewry, P., and Gutteridge, S., Eds.) pp 93−141, Cambridge University Press, Cambridge, United Kingdom.
54. Roffey, R. A., Kramer, D. M., Govindjee, and Sayre, R. T. (1994) *Biochim. Biophys. Acta 1185*, 257−270.
55. Nixon, P. J., and Diner, B. A. (1994) *Biochem. Soc. Trans. 22*, 338−343.
56. Chu, H.-A., Nguyen, A. P., and Debus, R. J. (1995) *Biochemistry 34*, 5859−5882.
57. Nixon, P. J., Trost, J. T., and Diner, B. A. (1992) *Biochemistry 31*, 10859−10871.

58. Debus, R. J., Campbell, K. A., Peloquin, J. M., Pham, D. P., and Britt, R. D. (2000) *Biochemistry 39*, 470−478.
59. Debus, R. J., Nguyen, A. P., and Conway, A. B. (1990) in *Current Research in Photosynthesis* (Baltscheffsky, M., Ed.) Vol. I, pp 829−832, Kluwer Academic Publishers, Dordrecht, The Netherlands.
60. Vermaas, W. F. J., Williams, J. G. K., and Arntzen, C. J. (1987) *Plant Mol. Biol. 8*, 317−326.
61. Vieira, J., and Messing, J. (1987) *Methods Enzymol. 153*, 3−11.
62. Reifler, M. J., Chisholm, D. A., Wang, J., Diner, B. A., and Brudvig, G. W. (1998) in *Photosynthesis, Mechanisms and Effects* (Garab, G., Ed.) Vol. II, pp 1189−1192, Kluwer Academic Publishers, Dordecht, The Netherlands.
63. Ho, S. N., Hunt, H. D., Horton, R. M., Pullen, J. K., and Pease, L. R. (1989) *Gene 77*, 51−59.
64. Horton, R. M., Hunt, H. D., Ho, S. N., Pullen, J. K., and Pease, L. R. (1989) *Gene 77*, 61−68.
65. Horton, R. M., Ho, S. N., Pullen, J. K., Hunt, H. D., Cai, Z., and Pease, L. R. (1993) *Methods Enzymol. 217*, 270−279.
66. Yin, J. C. P., Krebs, M. P., and Reznikoff, W. S. (1988) *J. Mol. Biol. 199*, 33−45.
67. Kaneko, T., and Tabata, S. (1997) *Plant Cell Physiol. 38*, 1171−1176.
68. Rippka, R., Deruelles, J., Waterbury, J. B., Herdman, M., and Stanier, R. Y. (1979) *J. Gen. Microbiol. 111*, 1−61.
69. Hays, A.-M. A., Vassiliev, I. R., Golbeck, J. H., and Debus, R. J. (1998) *Biochemistry 37*, 11352−11365.
70. Tang, X.-S., and Diner, B. A. (1994) *Biochemistry 33*, 4594−4603.
71. Berthold, D. A., Babcock, G. T., and Yocum, C. F. (1981) *FEBS Lett. 134*, 231−234.
72. Ford, R. C., and Evans, M. C. W. (1983) *FEBS Lett. 160*, 159−164.
73. Campbell, K. A., Gregor, W., Pham, D. P., Peloquin, J. M., Debus, R. J., and Britt, R. D. (1998) *Biochemistry 37*, 5039−5045.
74. Ghanotakis, D. F., Demetriou, D. M., and Yocum, C. F. (1987) *Biochim. Biophys. Acta 891*, 15−21.
75. Sturgeon, B. E., and Britt, R. D. (1992) *Rev. Sci. Instrum. 63*, 2187−2192.
76. Mims, W. B. (1984) *J. Magn. Reson. 59*, 291−306.
77. Rondeau, R. E. (1966) *J. Chem. Eng. Data 11*, 124.
78. Bricker, T. M., Morvant, J., Masri, N., Sutton, H. M., and Frankel, L. K. (1998) *Biochim. Biophys. Acta 1409*, 50−57.
79. Beck, W. F., de Paula, J. C., and Brudvig, G. W. (1986) *J. Am. Chem. Soc. 108*, 4018−4022.
80. Aasa, R., Andréasson, L.-E., Lagenfelt, G., and Vänngård, T. (1987) *FEBS Lett. 221*, 245−248.
81. Kirilovsky, D. L., Boussac, A. G. P., van Mieghem, F. J. E., Ducruet, J.-M. R. C., Sétif, P. R., Yu, J., Vermaas, W. F. J., and Rutherford, A. W. (1992) *Biochemistry 31*, 2099−2107.
82. Boussac, A., and Rutherford, A. W. (1988) *Biochemistry 27*, 3476−3483.
83. Campbell, K. A., Peloquin, J. M., Pham, D. P., Debus, R. J., and Britt, R. D. (1998) *J. Am. Chem. Soc. 120*, 447−448.
84. Li, Z.-L., Bricker, T. M., and Burnap, R. L. (2000) *Biochim. Biophys. Acta 1460*, 384−389.
85. Chu, H.-A., Debus, R. J., and Babcock, G. T. (2001) *Biochemistry 40*, 2312−2316.
86. Noguchi, T., and Sugiura, M. (2000) *Biochemistry 39*, 10943−10949.
87. Boussac, A., Sugiura, M., Inoue, Y., and Rutherford, A. W. (2000) *Biochemistry 39*, 13788−13799.
88. Britt, R. D., Zimmermann, J.-L., Sauer, K., and Klein, M. P. (1989) *J. Am. Chem. Soc. 111*, 3522−3532.
89. Stewart, D. H., and Brudvig, G. W. (1998) *Biochim. Biophys. Acta 1367*, 63−87.
90. Boussac, A., Deligiannakis, Y., and Rutherford, A. W. (1998) in *Photosynthesis: Mehanisms and Effects* (Garab, G., Ed.) Vol. II, pp 1233−1240, Kluwer Academic Publishers, Dordrecht, The Netherlands.
91. Seidler, A. (1996) *Biochim. Biophys. Acta 1277*, 35−60.
92. Mizusawa, N., Yamashita, T., and Miyao, M. (1999) *Biochim. Biophys. Acta 1410*, 273−286.
93. Nedbal, L., Samson, G., and Whitmarsh, J. (1992) *Proc. Natl. Acad. Sci. U.S.A. 89*, 7929−7933.
94. Barber, J., and De Las Rivas, J. (1993) *Proc. Natl. Acad. Sci. U.S.A. 90*, 10942−10946.
95. De Las Rivas, J., Klein, J., and Barber, J. (1995) *Photosynth. Res. 46*, 193−202.
96. Poulson, M., Samson, G., and Whitmarsh, J. (1995) *Biochemistry 34*, 10932−10938.
97. Kruk, J., and Strzalka, K. (2001) *J. Biol. Chem. 276*, 86−91.
98. Ghanotakis, D. F., and Yocum, C. F. (1986) *FEBS Lett. 197*, 244−248.
99. Boussac, A., Un, S., Horner, O., and Rutherford, A. W. (1998) *Biochemistry 37*, 4001−4007.
100. Boussac, A., Kuhl, H., Un, S., Rögner, M., and Rutherford, A. W. (1998) *Biochemistry 37*, 8995−9000.
101. Mims, W. B. (1972) *Phys. Rev. B 5*, 2409−2419.
102. Mims, W. B. (1972) *Phys. Rev. B 6*, 3543−3545.
103. Mims, W. B., and Peisach, J. (1989) in *Advanced EPR: Applications in Biology and Biochemistry* (Hoff, A. J., Ed.) pp 1−57, Elsevier Science Publishers, Amsterdam, The Netherlands.
104. Sundaramoorthy, M., Choudhury, K., Edwards, S. L., and Poulos, T. L. (1991) *J. Am. Chem. Soc. 113*, 7755−7757.
105. Choudhury, K., Sundaramoorthy, M., Mauro, J. M., and Poulos, T. L. (1992) *J. Biol. Chem. 267*, 25656−25659.
106. Choudhury, K., Sundaramoorthy, M., Hickman, A., Yonetani, T., Woehl, E., Dunn, M. F., and Poulos, T. L. (1994) *J. Biol. Chem. 269*, 20239−20249.
107. Balasubramanian, S., Carr, R. T., Bender, C. J., Peisach, J., and Benkovic, S. J. (1994) *Biochemistry 33*, 8532−8537.
108. Bender, C. J., Casimiro, D. R., Peisach, J., and Dyson, H. J. (1997) *J. Chem. Soc., Faraday Trans. 93*, 3967−3980.
109. Coremans, J. W. A., van Gastel, M., Poluektov, O. G., Groenen, E. J. J., den Blaauwen, T., Van Pouderoyen, G., Canters, G. W., Nar, H., Hammann, C., and Messerschmidt, A. (1995) *Chem. Phys. Lett. 235*, 202−210.
110. van Gastel, M., Coremans, J. W. A., Jeuken, L. J. C., Canters, G. W., and Groenen, E. J. J. (1998) *J. Phys. Chem. A 102*, 4462−4470.
111. Deligiannakis, Y., Louloudi, M., and Hadjiliadis, N. (2000) *Coord. Chem. Rev. 204*, 1−112.
112. Stallings, W. C., Pattridge, K. A., Strong, R. K., and Ludwig, M. L. (1985) *J. Biol. Chem. 260*, 16424−16432.
113. Zheng, M., and Dismukes, G. C. (1996) *Inorg. Chem. 35*, 3307−3319.
114. Lee, H.-I., Thrasher, K. S., Dean, D. R., Newton, W. E., and Hoffman, B. M. (1998) *Biochemistry 37*, 13370−13378.
115. DeRose, V. J., Kim, C.-H., Newton, W. E., Dean, D. R., and Hoffman, B. M. (1995) *Biochemistry 34*, 2809−2814.
116. Quillin, M. L., Arduini, R. M., Olson, J. S., and Phillips, G. N., Jr. (1993) *J. Mol. Biol. 234*, 140−155.
117. Haining, R. L., and McFadden, B. A. (1994) *Photosynth. Res. 41*, 349−356.
118. Britt, R. D., and Klein, M. P. (1992) in *Pulsed Magnetic Resonance: NMR, ESR, and Optics, a Recognition of E. L. Hahn* (Bagguley, D. M. S., Ed.) pp 361−376, Clarendon Press, Oxford, United Kingdom.
119. Sturgeon, B. E. (1994) Ph.D. Dissertation, University of California, Davis, CA.

BI002394C